Supporting Information

Computational Discovery of Stable Na-ion Sulfide Solid Electrolytes with High Conductivity at Room Temperature

Seong-Hoon Jang,[1,2] Randy Jalem,[2] and Yoshitaka Tateyama[2,3]*

[1] Institute for Materials Research, Tohoku University, 2-1-1 Katahira, Aoba-ku, Sendai, 980-8577, Japan

[2] Research Center for Energy and Environmental Materials (GREEN), National Institute for Materials Science (NIMS), 1-1 Namiki, Tsukuba, Ibaraki 305-0044, Japan

[3] Laboratory for Chemistry and Life Science, Tokyo Institute of Technology, 4259 Nagatsuta, Midori-ku, Yokohama, 226-8501, Japan

*Corresponding author: jang.seonghoon.b4@tohoku.ac.jp

Discussion S1 Details of sampling protocol

Sampling space. The space group for each Ω is as follows: Na_5AlS_4 (with the orthorhombic $Pbca$ symmetry),[1, 2] Na_5InS_4 (monoclinic $P2_1/m$),[3] $Na_{4.5}Al_{0.5}Si_{0.5}S_4$ (monoclinic Cc),[1] Na_4SiS_4 (orthorhombic $P2_12_12_1$),[1, 4-6] Na_4SnS_4 (tetragonal $P\bar{4}2_1c$),[7-9] Na_3VS_4 (tetragonal $P\bar{4}2_1c$),[10-12] and Na_3SbS_4 (tetragonal $P\bar{4}2_1c$).[1, 13-15]

Ewald summation sampling. 112 cases of $(M, M^{'}, \Omega)$ at $m = m^{'} = 0.5$ were taken in total: 105 cases of $Na_4M_{0.5}M'_{0.5}S_4$ for $v(M) = 3$ and $v(M^{'}) = 5$ and 7 cases of $Na_{3.5}Si_{0.5}Ta_{0.5}S_4$. We conducted supercell operations on the abovementioned parent structures. We modified the number of Na-ions when necessary, and replaced host metal ion sites with M and M'. This resulted in supercells with varying numbers of ion sites: 144 for $\Omega = Na_5AlS_4$, Na_5InS_4, $Na_{4.5}Al_{0.5}Si_{0.5}S_4$, Na_3VS_4, and Na_3SbS_4 and 216 for $\Omega = Na_4SiS_4$ and Na_4SnS_4 with $v(M) = 3$ and $v(M^{'}) = 5$; 136 for $\Omega = Na_5AlS_4$, Na_5InS_4, $Na_{4.5}Al_{0.5}Si_{0.5}S_4$, Na_4SnS_4, Na_3VS_4, and Na_3SbS_4 and 204 for Na_4SiS_4 with $Na_{3.5}Si_{0.5}Ta_{0.5}S_4$.

For each Ω with $v(M) = 3$ and $v(M^{'}) = 5$ (or with $Na_{3.5}Si_{0.5}Ta_{0.5}S_4$), a substantial number of random site arrangements was generated, ranging from $18{,}200$ to $623{,}551{,}500$ (from $33{,}124{,}000$ to $2{,}460{,}781{,}960$) and giving a total dataset size of $n_{data} = 5{,}290{,}074{,}920$. From these site arrangements, we selected less than 6 site arrangements with lowest Ewald Coulombic energies E_{Ewald} for each case of $Na_4M_{0.5}M'_{0.5}S_4$ or $Na_{3.5}Si_{0.5}Ta_{0.5}S_4$ ($n_{data} = 469$).[16-18] In the subsequent step of DFT geometry optimizations, we fully relaxed the site positions and lattice parameters for the selected site arrangements. The cell structure with the lowest DFT energy E_{DFT} or, equivalently, the lowest E_{hull}, was chosen as the representative sample for each case of $Na_4M_{0.5}M'_{0.5}S_4$ or $Na_{3.5}Si_{0.5}Ta_{0.5}S_4$ for the succeeding DFT-MD sampling ($n_{data} = 16$).

Geometry optimization with DFT. This step was performed by using the Vienna Ab Initio Simulation Package (VASP). We employed the generalized gradient approximation (GGA) and the projector augmented wave (PAW) method basis set.[19-23] The geometry optimizations included both site positions and lattice constants. Monkhorst-Pack k-grids were set at $2 \times 2 \times 2$,[24] and the kinetic energy cutoff of 520 eV was used. Convergence criteria of < 0.01 eV·Å^{-1} for forces and $< 10^{-5}$ eV·atom^{-1} for energy were applied. Some pseudopotentials included semicore electrons as valence states for specific elements: Ca, Sc, and Zr (semicore s electrons); Na, V, Nb, and Ta (p); and Ga, In, and Sn (d). For the other elements, standard pseudopotential forms were employed. Then, the lowest-energy structure sample for each investigated composition was selected for subsequent DFT-MD calculations, wherein we calculated E_{hull} for all the samples by using the Computational Phase Diagram App provided by MaterialsProject.org[25, 26] to verify their thermodynamic (meta)stability. Bandgap energies E_g were also examined for some of the samples by using Heyd-Scuseria-Ernzerhof hybrid functionals (HSE06) provided under VASP.[27]

DFT-MD for the single-temperature "long-time" diagnosis. The single-temperature "long-time" diagnosis was carried out at $T = 300$ K given the geometry-optimized cell structures described above. First, a total of $10{,}000$ DFT-MD steps (10 ps) were performed to ensure thermal equilibrations by using the Nosé-Hoover thermostat (NVT ensemble) implemented in VASP.[28, 29] Subsequently, DFT-MD production runs were executed for trajectory sampling over $\tau = 250$ ps (NVT). Throughout the DFT-MD calculations, $\Delta\tau = 1$ fs, a $1 \times 1 \times 1$ k-grid (that is, Γ only), and a kinetic energy cutoff of 400 eV were employed. The pseudopotentials were used in their standard forms except for Nb (with semicore p electrons), and the calculations were performed using the GGA and the PAW method basis set.[19-23]

From the sampled trajectories, the Na-ion self-diffusion coefficients $D_{Na,T} = M_s/(2d)$ at T were estimated by conducting regression analyses on the mean squared displacement (MSD) curves against sampled time intervals $\Delta\tau_{MSD}$; $D_{Na,T}$ was obtained as the slope M_s of the MSD-$\Delta\tau_{MSD}$ regression line at T, considering the three-dimensional nature of Na-ion diffusion ($d = 3$). Then, the Na-ion ionic conductivity $\sigma_{Na,T}$ at T is estimated by using the Nernst-Einstein equation

$$\sigma_{Na,T} = \frac{(z_{Na}F)^2\rho_{Na}}{RT}D_{Na,T}, \quad \text{(S1)}$$

where z_{Na} ($=+1$) is the valence for a Na-ion, ρ_{Na} is the Na-ion density, and F and R denote the Faraday constant and the gas constant, respectively.

DFT-MD for multi-temperature calculations. The multi-temperature DFT-MD calculations were conducted at $T = 500$, 600, 700, 800, and 900 K for Na_4SiS_4, $Na_4Ga_{0.125}Si_{0.75}P_{0.125}S_4$, $Na_4Ga_{0.25}Si_{0.5}P_{0.25}S_4$, $Na_4Ga_{0.375}Si_{0.25}P_{0.375}S_4$, $Na_4Ga_{0.5}P_{0.5}S_4$, $Na_{3.75}Ga_{0.375}P_{0.625}S_4$, $Na_{4.25}Ga_{0.625}P_{0.375}S_4$, $Na_{3.875}Si_{0.875}Ta_{0.125}S_4$, $Na_{3.75}Si_{0.75}Ta_{0.25}S_4$, $Na_{3.625}Si_{0.625}Ta_{0.375}S_4$, and $Na_{3.5}Si_{0.5}Ta_{0.5}S_4$ with $\Omega = Na_4SiS_4$. First, a total of $40{,}000$ DFT-MD steps (40 ps) were performed to achieve thermal and volume equilibrations by using the Langevin thermostat with the Parinello-Rahman algorithm (NpT ensemble) implemented in VASP.[30, 31] During this process, the averaged lattice constants were calculated over the last $10{,}000$ DFT-MD steps (30 - 40 ps) to account cell volumes expanded thermally. Subsequently, with the averaged lattice constants, thermal equilibration runs were repeated for $10{,}000$ DFT-MD steps (10 ps) under the Nosé-Hoover thermostat (NVT). Finally, product runs were conducted afterwards for trajectory sampling over $\tau = 100$ ps (NVT). Meanwhile, the choices of $\Delta\tau$, the k-grid, the kinetic energy cutoff, and the pseudopotentials and the post-process for $D_{Na,T}$ and $\sigma_{Na,T}$ were common to those of the DFT-MD for the single-temperature “long-time” diagnosis

Table S1 Lattice constants a, b, c, α, β, and γ, unit cell volumes V, and convex hull decomposition energies per atom E_{hull} for compositions $Na_4M_{0.5}M'_{0.5}S_4$ and $Na_{3.5}Si_{0.5}Ta_{0.5}S_4$ whose structures were relaxed by using DFT across various parent structures Ω

Composition	Composition per unit cell	Ω	a (Å)	b (Å)	c (Å)	α (°)	β (°)	γ (°)	V (Å^3)	E_{hull} (meV·atom^{-1})
$Na_4Al_{0.5}P_{0.5}S_4$	$Na_{64}Al_8P_8S_{64}$	Na_5AlS_4	11.563	14.190	21.618	91.693	89.528	90.045	3545.4	37.9
$Na_4Al_{0.5}P_{0.5}S_4$	$Na_{64}Al_8P_8S_{64}$	Na_5InS_4	13.887	17.765	14.446	89.422	86.947	89.851	3558.6	26.4
$Na_4Al_{0.5}P_{0.5}S_4$	$Na_{64}Al_8P_8S_{64}$	$Na_{4.5}Al_{0.5}Si_{0.5}S_4$	17.585	13.997	14.374	89.792	92.950	90.627	3533.2	23.7
$Na_4Al_{0.5}P_{0.5}S_4$	$Na_{96}Al_{12}P_{12}S_{96}$	Na_4SiS_4	41.870	8.917	13.857	89.953	89.529	90.035	5173.6	14.6
$Na_4Al_{0.5}P_{0.5}S_4$	$Na_{96}Al_{12}P_{12}S_{96}$	Na_4SnS_4	15.585	15.585	13.635	90.000	90.000	90.000	3311.6	24.6
$Na_4Al_{0.5}P_{0.5}S_4$	$Na_{64}Al_8P_8S_{64}$	Na_3VS_4	14.169	14.611	16.480	89.235	87.477	89.334	3407.6	65.1
$Na_4Al_{0.5}P_{0.5}S_4$	$Na_{64}Al_8P_8S_{64}$	Na_3SbS_4	19.832	13.103	20.902	88.821	89.960	89.890	5430.5	43.5
$Na_4Al_{0.5}V_{0.5}S_4$	$Na_{64}Al_8V_8S_{64}$	Na_5AlS_4	11.681	14.390	21.401	90.865	89.541	89.608	3596.9	39.7
$Na_4Al_{0.5}V_{0.5}S_4$	$Na_{64}Al_8V_8S_{64}$	Na_5InS_4	13.926	17.642	14.553	88.839	87.345	89.680	3570.6	33.5
$Na_4Al_{0.5}V_{0.5}S_4$	$Na_{64}Al_8V_8S_{64}$	$Na_{4.5}Al_{0.5}Si_{0.5}S_4$	17.772	13.744	14.381	89.556	93.448	89.816	3506.0	24.1
$Na_4Al_{0.5}V_{0.5}S_4$	$Na_{96}Al_{12}V_{12}S_{96}$	Na_4SiS_4	41.903	8.7802	14.081	89.999	90.011	90.023	5180.7	16.8
$Na_4Al_{0.5}V_{0.5}S_4$	$Na_{96}Al_{12}V_{12}S_{96}$	Na_4SnS_4	15.586	15.586	13.735	90.000	90.000	90.000	3336.8	30.2
$Na_4Al_{0.5}V_{0.5}S_4$	$Na_{64}Al_8V_8S_{64}$	Na_3VS_4	14.909	14.213	16.334	88.085	90.759	89.052	3458.4	55.6
$Na_4Al_{0.5}V_{0.5}S_4$	$Na_{64}Al_8V_8S_{64}$	Na_3SbS_4	19.673	12.940	21.359	89.371	89.724	90.815	5436.3	46.4
$Na_4Al_{0.5}Nb_{0.5}S_4$	$Na_{64}Al_8Nb_8S_{64}$	Na_5AlS_4	11.987	14.491	21.556	90.262	89.535	89.453	3744.1	36.2
$Na_4Al_{0.5}Nb_{0.5}S_4$	$Na_{64}Al_8Nb_8S_{64}$	Na_5InS_4	13.728	17.710	15.066	88.779	87.839	89.545	3659.5	25.2
$Na_4Al_{0.5}Nb_{0.5}S_4$	$Na_{64}Al_8Nb_8S_{64}$	$Na_{4.5}Al_{0.5}Si_{0.5}S_4$	17.908	13.925	14.502	89.564	93.126	89.544	3610.7	17.8
$Na_4Al_{0.5}Nb_{0.5}S_4$	$Na_{96}Al_{12}Nb_{12}S_{96}$	Na_4SiS_4	42.197	8.951	14.154	90.032	90.194	90.051	5346.0	17.2
$Na_4Al_{0.5}Nb_{0.5}S_4$	$Na_{96}Al_{12}Nb_{12}S_{96}$	Na_4SnS_4	15.659	15.659	13.864	90.000	90.000	90.000	3399.4	20.1
$Na_4Al_{0.5}Nb_{0.5}S_4$	$Na_{64}Al_8Nb_8S_{64}$	Na_3VS_4	14.697	14.940	16.468	89.435	88.221	90.044	3613.9	40.1
$Na_4Al_{0.5}Nb_{0.5}S_4$	$Na_{64}Al_8Nb_8S_{64}$	Na_3SbS_4	20.157	13.358	20.970	89.887	89.863	89.381	5646.0	52.9
$Na_4Al_{0.5}Sb_{0.5}S_4$	$Na_{64}Al_8Sb_8S_{64}$	Na_5AlS_4	11.928	14.315	21.773	90.646	89.682	89.780	3717.4	39.7
$Na_4Al_{0.5}Sb_{0.5}S_4$	$Na_{64}Al_8Sb_8S_{64}$	Na_5InS_4	13.783	17.861	15.167	87.904	87.622	88.588	3727.1	31.4
$Na_4Al_{0.5}Sb_{0.5}S_4$	$Na_{96}Al_{12}Sb_{12}S_{96}$	$Na_{4.5}Al_{0.5}Si_{0.5}S_4$	17.853	14.046	14.748	89.831	92.665	89.872	3694.3	24.0
$Na_4Al_{0.5}Sb_{0.5}S_4$	$Na_{96}Al_{12}Sb_{12}S_{96}$	Na_4SiS_4	42.002	9.1901	14.060	90.044	90.035	90.017	5427.3	26.9
$Na_4Al_{0.5}Sb_{0.5}S_4$	$Na_{64}Al_8Sb_8S_{64}$	Na_4SnS_4	15.738	15.738	13.862	90.000	90.000	90.000	3433.5	13.9
$Na_4Al_{0.5}Sb_{0.5}S_4$	$Na_{64}Al_8Sb_8S_{64}$	Na_3VS_4	15.221	15.015	15.946	87.826	88.415	91.302	3639.5	50.6
$Na_4Al_{0.5}Sb_{0.5}S_4$	$Na_{64}Al_8Sb_8S_{64}$	Na_3SbS_4	20.680	13.613	20.337	89.405	89.142	89.863	5724.2	54.9
$Na_4Al_{0.5}Ta_{0.5}S_4$	$Na_{64}Al_8Ta_8S_{64}$	Na_5AlS_4	12.098	14.542	21.711	90.707	87.790	89.364	3816.4	43.7
$Na_4Al_{0.5}Ta_{0.5}S_4$	$Na_{64}Al_8Ta_8S_{64}$	Na_5InS_4	13.759	17.727	15.062	88.815	87.823	89.575	3670.4	27.9
$Na_4Al_{0.5}Ta_{0.5}S_4$	$Na_{96}Al_{12}Ta_{12}S_{96}$	$Na_{4.5}Al_{0.5}Si_{0.5}S_4$	17.917	13.926	14.501	89.558	93.144	89.582	3612.5	20.0
$Na_4Al_{0.5}Ta_{0.5}S_4$	$Na_{96}Al_{12}Ta_{12}S_{96}$	Na_4SiS_4	42.228	8.9538	14.139	90.029	90.229	90.064	5346.1	19.4
$Na_4Al_{0.5}Ta_{0.5}S_4$	$Na_{64}Al_8Ta_8S_{64}$	Na_4SnS_4	15.672	15.671	13.849	89.997	89.999	89.998	3401.4	22.6
$Na_4Al_{0.5}Ta_{0.5}S_4$	$Na_{64}Al_8Ta_8S_{64}$	Na_3VS_4	14.692	14.960	16.489	89.559	88.297	90.319	3622.4	41.1
$Na_4Al_{0.5}Ta_{0.5}S_4$	$Na_{64}Al_8Ta_8S_{64}$	Na_3SbS_4	19.895	13.225	21.368	88.790	89.093	91.101	5619.2	45.6
$Na_4Ga_{0.5}P_{0.5}S_4$	$Na_{64}Ga_8P_8S_{64}$	Na_5AlS_4	11.960	14.307	21.436	90.925	89.009	89.485	3666.7	52.6
$Na_4Ga_{0.5}P_{0.5}S_4$	$Na_{64}Ga_8P_8S_{64}$	Na_5InS_4	13.735	17.843	14.684	88.868	86.897	89.170	3592.3	31.0
$Na_4Ga_{0.5}P_{0.5}S_4$	$Na_{64}Ga_8P_8S_{64}$	$Na_{4.5}Al_{0.5}Si_{0.5}S_4$	17.801	13.710	14.375	89.591	93.334	89.737	3502.3	25.1
$Na_4Ga_{0.5}P_{0.5}S_4$	$Na_{96}Ga_{12}P_{12}S_{96}$	Na_4SiS_4	41.764	8.977	13.873	89.966	89.739	89.986	5201.4	15.8
$Na_4Ga_{0.5}P_{0.5}S_4$	$Na_{96}Ga_{12}P_{12}S_{96}$	Na_4SnS_4	15.582	15.582	13.659	90.000	90.000	90.000	3316.3	23.8
$Na_4Ga_{0.5}P_{0.5}S_4$	$Na_{64}Ga_8P_8S_{64}$	Na_3VS_4	14.571	14.546	16.057	88.841	89.370	89.650	3402.3	63.4
$Na_4Ga_{0.5}P_{0.5}S_4$	$Na_{64}Ga_8P_8S_{64}$	Na_3SbS_4	20.571	13.426	20.179	89.362	89.607	88.852	5571.5	66.7
$Na_4Ga_{0.5}V_{0.5}S_4$	$Na_{64}Ga_8V_8S_{64}$	Na_5AlS_4	11.769	14.428	21.410	90.638	89.471	89.463	3634.9	43.2
$Na_4Ga_{0.5}V_{0.5}S_4$	$Na_{64}Ga_8V_8S_{64}$	Na_5InS_4	13.843	17.635	14.740	89.100	88.044	89.838	3595.9	41.7
$Na_4Ga_{0.5}V_{0.5}S_4$	$Na_{64}Ga_8V_8S_{64}$	$Na_{4.5}Al_{0.5}Si_{0.5}S_4$	17.809	13.752	14.420	89.586	93.435	89.762	3525.1	26.2
$Na_4Ga_{0.5}V_{0.5}S_4$	$Na_{96}Ga_{12}V_{12}S_{96}$	Na_4SiS_4	42.019	8.8071	14.050	89.991	90.034	90.029	5199.5	17.3
$Na_4Ga_{0.5}V_{0.5}S_4$	$Na_{96}Ga_{12}V_{12}S_{96}$	Na_4SnS_4	15.589	15.589	13.770	90.000	90.000	90.000	3346.4	28.6
$Na_4Ga_{0.5}V_{0.5}S_4$	$Na_{64}Ga_8V_8S_{64}$	Na_3VS_4	14.478	14.124	16.616	88.897	90.434	89.331	3396.5	70.4
$Na_4Ga_{0.5}V_{0.5}S_4$	$Na_{64}Ga_8V_8S_{64}$	Na_3SbS_4	19.964	13.071	21.228	90.423	90.478	89.628	5538.9	57.7
$Na_4Ga_{0.5}Nb_{0.5}S_4$	$Na_{64}Ga_8Nb_8S_{64}$	Na_5AlS_4	12.035	14.469	21.566	90.413	89.531	89.427	3754.9	37.3
$Na_4Ga_{0.5}Nb_{0.5}S_4$	$Na_{64}Ga_8Nb_8S_{64}$	Na_5InS_4	14.050	17.925	14.700	88.476	86.152	89.465	3692.2	20.5
$Na_4Ga_{0.5}Nb_{0.5}S_4$	$Na_{64}Ga_8Nb_8S_{64}$	$Na_{4.5}Al_{0.5}Si_{0.5}S_4$	17.893	13.969	14.593	90.061	93.354	90.129	3641.1	23.1
$Na_4Ga_{0.5}Nb_{0.5}S_4$	$Na_{96}Ga_{12}Nb_{12}S_{96}$	Na_4SiS_4	42.238	8.9891	14.132	90.023	90.161	90.052	5365.7	17.7
$Na_4Ga_{0.5}Nb_{0.5}S_4$	$Na_{96}Ga_{12}Nb_{12}S_{96}$	Na_4SnS_4	15.684	15.684	13.873	90.000	90.000	90.000	3412.5	18.2
$Na_4Ga_{0.5}Nb_{0.5}S_4$	$Na_{64}Ga_8Nb_8S_{64}$	Na_3VS_4	14.938	14.408	16.596	89.045	90.590	88.645	3570.4	50.0
$Na_4Ga_{0.5}Nb_{0.5}S_4$	$Na_{64}Ga_8Nb_8S_{64}$	Na_3SbS_4	20.081	13.156	21.388	90.195	89.683	91.129	5649.0	44.8
$Na_4Ga_{0.5}Sb_{0.5}S_4$	$Na_{64}Ga_8Sb_8S_{64}$	Na_5AlS_4	12.239	14.404	21.927	90.946	87.669	89.082	3861.2	53.8
$Na_4Ga_{0.5}Sb_{0.5}S_4$	$Na_{64}Ga_8Sb_8S_{64}$	Na_5InS_4	13.728	17.960	15.165	89.420	88.291	89.607	3736.8	36.1
$Na_4Ga_{0.5}Sb_{0.5}S_4$	$Na_{96}Ga_{12}Sb_{12}S_{96}$	$Na_{4.5}Al_{0.5}Si_{0.5}S_4$	17.917	14.080	14.795	89.799	92.441	89.890	3728.8	29.7
$Na_4Ga_{0.5}Sb_{0.5}S_4$	$Na_{96}Ga_{12}Sb_{12}S_{96}$	Na_4SiS_4	42.082	9.1991	14.022	90.019	89.389	90.017	5427.8	31.2
$Na_4Ga_{0.5}Sb_{0.5}S_4$	$Na_{64}Ga_8Sb_8S_{64}$	Na_4SnS_4	15.755	15.755	13.895	90.000	90.000	90.000	3449.2	15.5
$Na_4Ga_{0.5}Sb_{0.5}S_4$	$Na_{64}Ga_8Sb_8S_{64}$	Na_3VS_4	14.988	14.720	16.401	89.586	86.820	89.398	3612.6	61.0

$Na_4Ga_{0.5}Sb_{0.5}S_4$	$Na_{64}Ga_8Sb_8S_{64}$	Na_3SbS_4	20.325	13.580	20.759	90.656	89.115	90.377	5728.5	44.2
$Na_4Ga_{0.5}Ta_{0.5}S_4$	$Na_{64}Ga_8Ta_8S_{64}$	Na_5AlS_4	12.176	14.211	21.575	91.189	89.572	89.006	3731.9	35.9
$Na_4Ga_{0.5}Ta_{0.5}S_4$	$Na_{64}Ga_8Ta_8S_{64}$	Na_5InS_4	13.968	17.881	14.766	88.324	87.413	89.145	3682.3	27.7
$Na_4Ga_{0.5}Ta_{0.5}S_4$	$Na_{96}Ga_{12}Ta_{12}S_{96}$	$Na_{4.5}Al_{0.5}Si_{0.5}S_4$	17.942	13.951	14.539	89.594	93.122	89.533	3633.7	22.1
$Na_4Ga_{0.5}Ta_{0.5}S_4$	$Na_{96}Ga_{12}Ta_{12}S_{96}$	Na_4SiS_4	42.303	8.9968	14.106	90.028	90.293	90.068	5368.5	19.7
$Na_4Ga_{0.5}Ta_{0.5}S_4$	$Na_{64}Ga_8Ta_8S_{64}$	Na_4SnS_4	15.698	15.698	13.896	90.000	90.000	90.000	3424.6	20.6
$Na_4Ga_{0.5}Ta_{0.5}S_4$	$Na_{64}Ga_8Ta_8S_{64}$	Na_3VS_4	14.759	14.822	16.418	89.175	87.358	89.305	3587.1	56.3
$Na_4Ga_{0.5}Ta_{0.5}S_4$	$Na_{64}Ga_8Ta_8S_{64}$	Na_3SbS_4	19.927	13.099	21.395	91.280	90.020	90.630	5582.6	44.5
$Na_4In_{0.5}P_{0.5}S_4$	$Na_{64}In_8P_8S_{64}$	Na_5AlS_4	11.758	14.352	21.597	92.324	90.350	89.461	3641.1	51.8
$Na_4In_{0.5}P_{0.5}S_4$	$Na_{64}In_8P_8S_{64}$	Na_5InS_4	13.861	18.128	14.778	89.377	86.092	89.224	3704.0	33.7
$Na_4In_{0.5}P_{0.5}S_4$	$Na_{64}In_8P_8S_{64}$	$Na_{4.5}Al_{0.5}Si_{0.5}S_4$	17.824	14.209	14.613	90.834	94.312	90.583	3689.9	42.7
$Na_4In_{0.5}P_{0.5}S_4$	$Na_{96}In_{12}P_{12}S_{96}$	Na_4SiS_4	42.123	9.1717	13.892	89.908	90.168	90.030	5366.9	31.1
$Na_4In_{0.5}P_{0.5}S_4$	$Na_{96}In_{12}P_{12}S_{96}$	Na_4SnS_4	15.933	15.933	13.645	90.000	90.000	90.000	3463.9	30.8
$Na_4In_{0.5}P_{0.5}S_4$	$Na_{64}In_8P_8S_{64}$	Na_3VS_4	14.500	15.823	15.860	88.948	92.706	88.796	3633.4	55.1
$Na_4In_{0.5}P_{0.5}S_4$	$Na_{64}In_8P_8S_{64}$	Na_3SbS_4	20.314	13.460	20.538	90.131	90.212	89.445	5615.3	59.8
$Na_4In_{0.5}V_{0.5}S_4$	$Na_{64}In_8V_8S_{64}$	Na_5AlS_4	11.772	14.432	21.640	91.785	89.711	89.663	3674.7	55.4
$Na_4In_{0.5}V_{0.5}S_4$	$Na_{64}In_8V_8S_{64}$	Na_5InS_4	13.691	17.872	15.051	89.244	87.699	89.753	3679.4	44.4
$Na_4In_{0.5}V_{0.5}S_4$	$Na_{64}In_8V_8S_{64}$	$Na_{4.5}Al_{0.5}Si_{0.5}S_4$	17.978	13.904	14.606	89.676	93.832	89.813	3642.7	44.8
$Na_4In_{0.5}V_{0.5}S_4$	$Na_{96}In_{12}V_{12}S_{96}$	Na_4SiS_4	42.274	9.0120	14.086	89.936	90.260	90.002	5366.3	37.1
$Na_4In_{0.5}V_{0.5}S_4$	$Na_{96}In_{12}V_{12}S_{96}$	Na_4SnS_4	15.830	15.830	13.822	90.000	90.000	90.000	3463.7	35.9
$Na_4In_{0.5}V_{0.5}S_4$	$Na_{64}In_8V_8S_{64}$	Na_3VS_4	15.310	14.424	16.386	87.890	90.168	87.426	3612.3	68.6
$Na_4In_{0.5}V_{0.5}S_4$	$Na_{64}In_8V_8S_{64}$	Na_3SbS_4	20.277	13.405	21.038	90.621	89.971	89.915	5718.0	70.3
$Na_4In_{0.5}Nb_{0.5}S_4$	$Na_{64}In_8Nb_8S_{64}$	Na_5AlS_4	12.341	14.497	21.644	91.067	89.627	89.418	3871.3	53.8
$Na_4In_{0.5}Nb_{0.5}S_4$	$Na_{64}In_8Nb_8S_{64}$	Na_5InS_4	13.734	17.925	15.315	89.199	88.186	89.796	3767.8	34.8
$Na_4In_{0.5}Nb_{0.5}S_4$	$Na_{64}In_8Nb_8S_{64}$	$Na_{4.5}Al_{0.5}Si_{0.5}S_4$	18.133	14.160	14.717	89.714	93.364	89.577	3772.0	37.3
$Na_4In_{0.5}Nb_{0.5}S_4$	$Na_{96}In_{12}Nb_{12}S_{96}$	Na_4SnS_4	15.836	15.836	13.969	90.000	90.000	90.000	3503.3	23.5
$Na_4In_{0.5}Nb_{0.5}S_4$	$Na_{64}In_8Nb_8S_{64}$	Na_3VS_4	14.799	14.470	17.068	89.110	88.201	88.816	3651.8	64.4
$Na_4In_{0.5}Nb_{0.5}S_4$	$Na_{64}In_8Nb_8S_{64}$	Na_3SbS_4	20.598	13.690	20.627	89.555	90.625	90.787	5815.5	58.1
$Na_4In_{0.5}Sb_{0.5}S_4$	$Na_{64}In_8Sb_8S_{64}$	Na_5AlS_4	12.390	14.411	21.110	90.680	89.885	89.314	3768.8	48.7
$Na_4In_{0.5}Sb_{0.5}S_4$	$Na_{64}In_8Sb_8S_{64}$	Na_5InS_4	13.744	18.116	15.357	89.189	87.797	89.721	3820.6	37.5
$Na_4In_{0.5}Sb_{0.5}S_4$	$Na_{96}In_{12}Sb_{12}S_{96}$	$Na_{4.5}Al_{0.5}Si_{0.5}S_4$	18.257	14.280	14.711	89.514	92.722	89.247	3830.7	44.1
$Na_4In_{0.5}Sb_{0.5}S_4$	$Na_{96}In_{12}Sb_{12}S_{96}$	Na_4SiS_4	42.153	9.4950	14.132	89.886	90.249	90.065	5656.0	36.6
$Na_4In_{0.5}Sb_{0.5}S_4$	$Na_{64}In_8Sb_8S_{64}$	Na_4SnS_4	15.916	15.916	13.957	90.000	90.000	90.000	3535.6	17.4
$Na_4In_{0.5}Sb_{0.5}S_4$	$Na_{64}In_8Sb_8S_{64}$	Na_3VS_4	14.857	15.198	16.623	89.589	87.892	89.608	3750.7	56.7
$Na_4In_{0.5}Sb_{0.5}S_4$	$Na_{64}In_8Sb_8S_{64}$	Na_3SbS_4	20.936	13.919	20.249	90.720	88.452	89.507	5897.6	60.0
$Na_4In_{0.5}Ta_{0.5}S_4$	$Na_{64}In_8Ta_8S_{64}$	Na_5AlS_4	12.350	14.500	21.647	91.009	89.503	89.417	3875.4	56.3
$Na_4In_{0.5}Ta_{0.5}S_4$	$Na_{64}In_8Ta_8S_{64}$	Na_5InS_4	13.765	17.962	15.279	89.131	87.971	89.767	3775.0	36.8
$Na_4In_{0.5}Ta_{0.5}S_4$	$Na_{96}In_{12}Ta_{12}S_{96}$	$Na_{4.5}Al_{0.5}Si_{0.5}S_4$	18.136	14.143	14.729	89.680	93.319	89.586	3771.5	39.9
$Na_4In_{0.5}Ta_{0.5}S_4$	$Na_{96}In_{12}Ta_{12}S_{96}$	Na_4SiS_4	42.515	9.2180	14.184	89.963	90.513	90.026	5558.5	38.8
$Na_4In_{0.5}Ta_{0.5}S_4$	$Na_{64}In_8Ta_8S_{64}$	Na_4SnS_4	15.845	15.845	13.970	90.000	90.000	90.000	3507.2	26.0
$Na_4In_{0.5}Ta_{0.5}S_4$	$Na_{64}In_8Ta_8S_{64}$	Na_3VS_4	14.899	14.593	16.949	89.268	88.186	88.355	3681.4	62.3
$Na_4In_{0.5}Ta_{0.5}S_4$	$Na_{64}In_8Ta_8S_{64}$	Na_3SbS_4	21.081	13.973	20.244	89.628	87.973	89.403	5959.4	75.4
$Na_{3.5}Si_{0.5}Ta_{0.5}S_4$	$Na_{56}Si_8Ta_8S_{64}$	Na_5AlS_4	11.602	14.197	22.060	90.395	91.871	90.771	3631.3	44.7
$Na_{3.5}Si_{0.5}Ta_{0.5}S_4$	$Na_{56}Si_8Ta_8S_{64}$	Na_5InS_4	13.625	18.213	14.391	90.715	86.832	91.114	3565.0	30.6
$Na_{3.5}Si_{0.5}Ta_{0.5}S_4$	$Na_{56}Si_8Ta_8S_{64}$	$Na_{4.5}Al_{0.5}Si_{0.5}S_4$	17.824	13.896	14.345	91.525	93.518	90.139	3545.0	31.7
$Na_{3.5}Si_{0.5}Ta_{0.5}S_4$	$Na_{84}Si_{12}Ta_{12}S_{96}$	Na_4SiS_4	41.654	8.9369	14.080	90.072	89.220	90.088	5241.0	24.1
$Na_{3.5}Si_{0.5}Ta_{0.5}S_4$	$Na_{56}Si_8Ta_8S_{64}$	Na_4SnS_4	15.802	15.445	13.845	90.360	90.620	89.424	3378.6	24.3
$Na_{3.5}Si_{0.5}Ta_{0.5}S_4$	$Na_{56}Si_8Ta_8S_{64}$	Na_3VS_4	14.192	13.926	16.324	89.917	89.817	89.664	3226.1	42.6

Table S2 Na-ion conductivity $\sigma_{Na,T}$ (in S·cm^{-1}) and Na-ion self-diffusion coefficient $D_{Na,T}$ (in cm^2·s^{-1}) for the 11 compositions adopted in the multi-temperature diagnosis with $\Delta\tau = 1$ fs, $\tau = 100$ ps, and $T = 500$, 600, 700, 800, and 800 K ("-" denotes the absence of observed Na-ion migrations). By extrapolating the values in the Arrhenius plots [see Figures 1(i) and 2(h)], Na-ion activation energies E_a and $\sigma_{Na,300K}$ were estimated as well. In E_a, the standard errors are presented. In the first row, the compositions per unit cell are presented in parentheses.

Composition	$\sigma_{Na,300K}$ ($D_{Na,300K}$)	$\sigma_{Na,500K}$ ($D_{Na,500K}$)	$\sigma_{Na,600K}$ ($D_{Na,600K}$)	$\sigma_{Na,700K}$ ($D_{Na,700K}$)	$\sigma_{Na,800K}$ ($D_{Na,800K}$)	$\sigma_{Na,900K}$ ($D_{Na,900K}$)	E_a (meV)
Na_4SiS_4 ($Na_{96}Si_{24}S_{96}$)	2.57×10^{-15} (2.00×10^{-20})	–	7.01×10^{-5} (1.26×10^{-9})	3.48×10^{-4} (7.43×10^{-9})	1.38×10^{-2} (3.40×10^{-7})	1.16×10^{-1} (3.27×10^{-6})	1250 ± 145
$Na_4Ga_{0.125}Si_{0.75}P_{0.125}S_4$ ($Na_{96}Ga_3Si_{18}P_3S_{96}$)	2.26×10^{-11} (1.84×10^{-16})	4.47×10^{-5} (6.69×10^{-10})	–	1.14×10^{-2} (2.45×10^{-7})	1.98×10^{-1} (4.99×10^{-6})	4.11×10^{-1} (1.18×10^{-5})	965 ± 43.1
$Na_4Ga_{0.25}Si_{0.5}P_{0.25}S_4$ ($Na_{96}Ga_6Si_{12}P_6S_{96}$)	9.48×10^{-9} (7.89×10^{-14})	5.11×10^{-4} (7.73×10^{-9})	7.39×10^{-3} (1.35×10^{-7})	1.66×10^{-1} (3.63×10^{-6})	1.25×10^{-1} (3.15×10^{-6})	7.13×10^{-1} (2.05×10^{-5})	747 ± 88.1
$Na_4Ga_{0.375}Si_{0.25}P_{0.375}S_4$ ($Na_{96}Ga_9Si_6P_9S_{96}$)	6.03×10^{-11} (4.89×10^{-16})	4.52×10^{-5} (6.83×10^{-10})	1.04×10^{-2} (1.92×10^{-7})	1.88×10^{-2} (4.07×10^{-7})	2.12×10^{-1} (5.39×10^{-6})	7.08×10^{-1} (2.07×10^{-5})	948 ± 111
$Na_4Ga_{0.5}P_{0.5}S_4$ ($Na_{96}Ga_{12}P_{12}S_{96}$)	9.71×10^{-4} (7.92×10^{-9})	7.00×10^{-2} (1.07×10^{-6})	1.51×10^{-1} (2.78×10^{-6})	1.48×10^{-1} (3.28×10^{-6})	6.39×10^{-1} (1.65×10^{-5})	8.24×10^{-1} (2.41×10^{-5})	297 ± 56.3
$Na_{3.75}Ga_{0.375}P_{0.625}S_4$ ($Na_{90}Ga_9P_{15}S_{96}$)	2.07×10^{-3} (1.77×10^{-8})	1.19×10^{-1} (1.91×10^{-6})	2.77×10^{-1} (5.41×10^{-6})	4.35×10^{-1} (1.02×10^{-5})	9.44×10^{-1} (2.55×10^{-5})	1.30×10^{0} (4.07×10^{-5})	290 ± 18.0
$Na_{4.25}Ga_{0.625}P_{0.375}S_4$ ($Na_{102}Ga_{15}P_9S_{96}$)	6.57×10^{-4} (5.26×10^{-9})	4.96×10^{-2} (7.23×10^{-7})	1.83×10^{-1} (3.27×10^{-6})	2.61×10^{-1} (5.47×10^{-6})	4.52×10^{-1} (1.10×10^{-5})	8.61×10^{-1} (2.41×10^{-5})	316 ± 22.6
$Na_{3.875}Si_{0.875}Ta_{0.125}S_4$ ($Na_{93}Si_{21}Ta_3S_{96}$)	4.93×10^{-5} (4.22×10^{-10})	2.06×10^{-2} (3.19×10^{-7})	6.53×10^{-2} (1.24×10^{-6})	1.47×10^{-1} (3.30×10^{-6})	4.06×10^{-1} (1.05×10^{-5})	8.40×10^{-1} (2.48×10^{-5})	413 ± 27.4
$Na_{3.75}Si_{0.75}Ta_{0.25}S_4$ ($Na_{90}Si_{18}Ta_6S_{96}$)	2.36×10^{-3} (2.10×10^{-8})	8.62×10^{-2} (1.39×10^{-6})	1.38×10^{-1} (2.72×10^{-6})	9.09×10^{-2} (2.11×10^{-6})	4.26×10^{-1} (1.14×10^{-5})	6.83×10^{-1} (2.09×10^{-5})	246 ± 77.5
$Na_{3.625}Si_{0.625}Ta_{0.375}S_4$ ($Na_{87}Si_{15}Ta_9S_{96}$)	4.53×10^{-3} (4.25×10^{-8})	1.12×10^{-1} (1.91×10^{-6})	4.70×10^{-1} (9.75×10^{-6})	3.78×10^{-1} (9.23×10^{-6})	7.64×10^{-1} (2.14×10^{-5})	1.02×10^{0} (3.32×10^{-5})	252 ± 40.8
$Na_{3.5}Si_{0.5}Ta_{0.5}S_4$ ($Na_{84}Al_{12}Ta_{12}S_{96}$)	1.35×10^{-2} (1.27×10^{-7})	2.53×10^{-1} (4.47×10^{-6})	3.90×10^{-1} (8.39×10^{-6})	5.34×10^{-1} (1.35×10^{-5})	1.03×10^{0} (3.07×10^{-5})	1.23×10^{0} (4.22×10^{-5})	215 ± 21.7

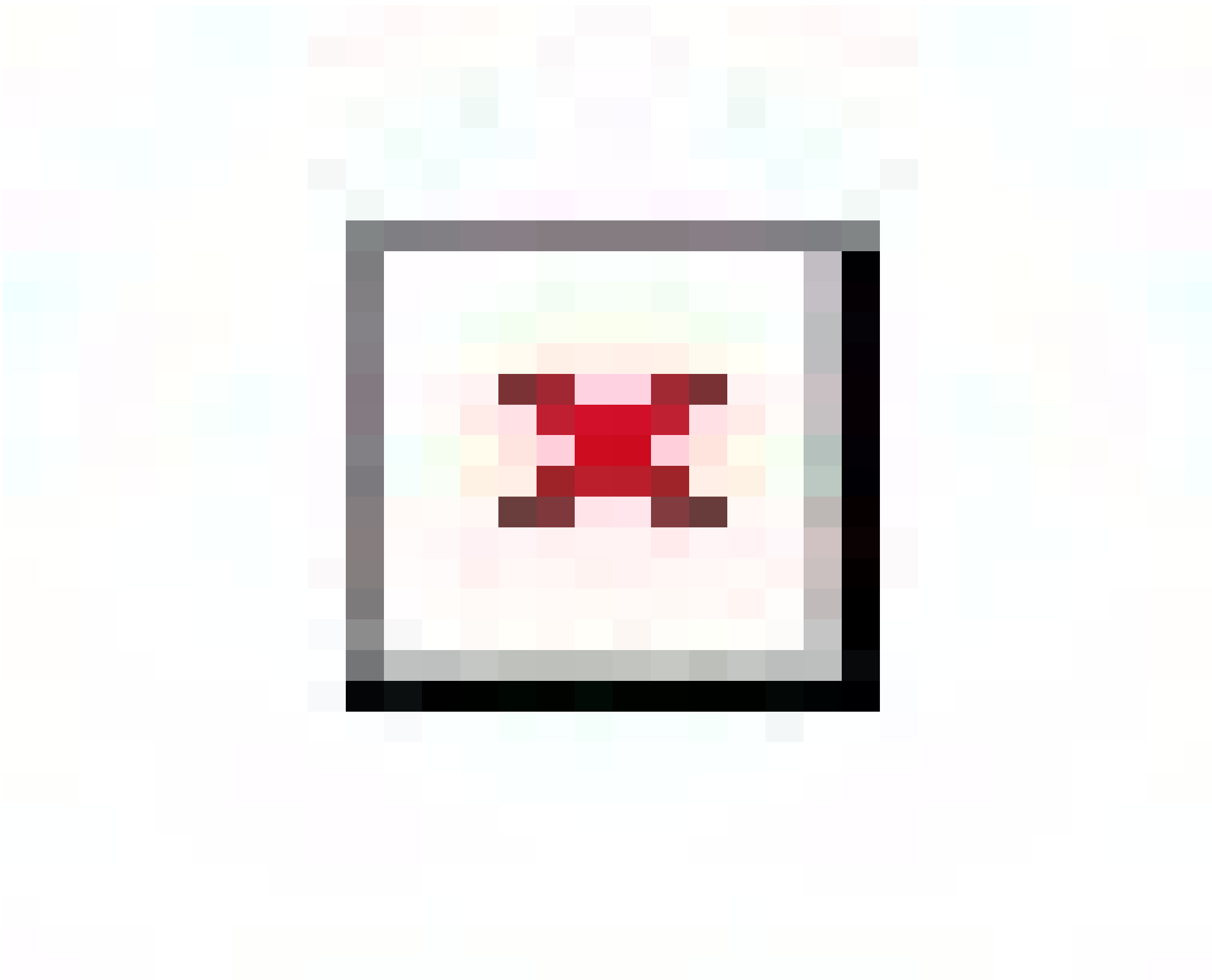

Figure S1 Mean squared displacement (MSD) curves against sampled time intervals $\Delta\tau_{MSD}$ given by the multi-temperature diagnosis (with $\Delta\tau = 1$ fs and $\tau = 100$ ps at $T = 500$, 600, 700, 800, and 900 K) for the seven samples within $(M, M^{'}, \Omega) = (Ga, P, Na_4SiS_4)$: (a) Na_4SiS_4, (b) $Na_4Ga_{0.125}Si_{0.75}P_{0.125}S_4$, (c) $Na_4Ga_{0.25}Si_{0.5}P_{0.25}S_4$, (d) $Na_4Ga_{0.375}Si_{0.25}P_{0.375}S_4$, (e) $Na_4Ga_{0.5}P_{0.5}S_4$, (f) $Na_{3.75}Ga_{0.375}P_{0.625}S_4$, and (g) $Na_{4.25}Ga_{0.625}P_{0.375}S_4$. The dashed lines with slopes represent regression analyses, and the insets present the trajectory density plot at $T =$ 500 K represented by yellow isosurfaces.

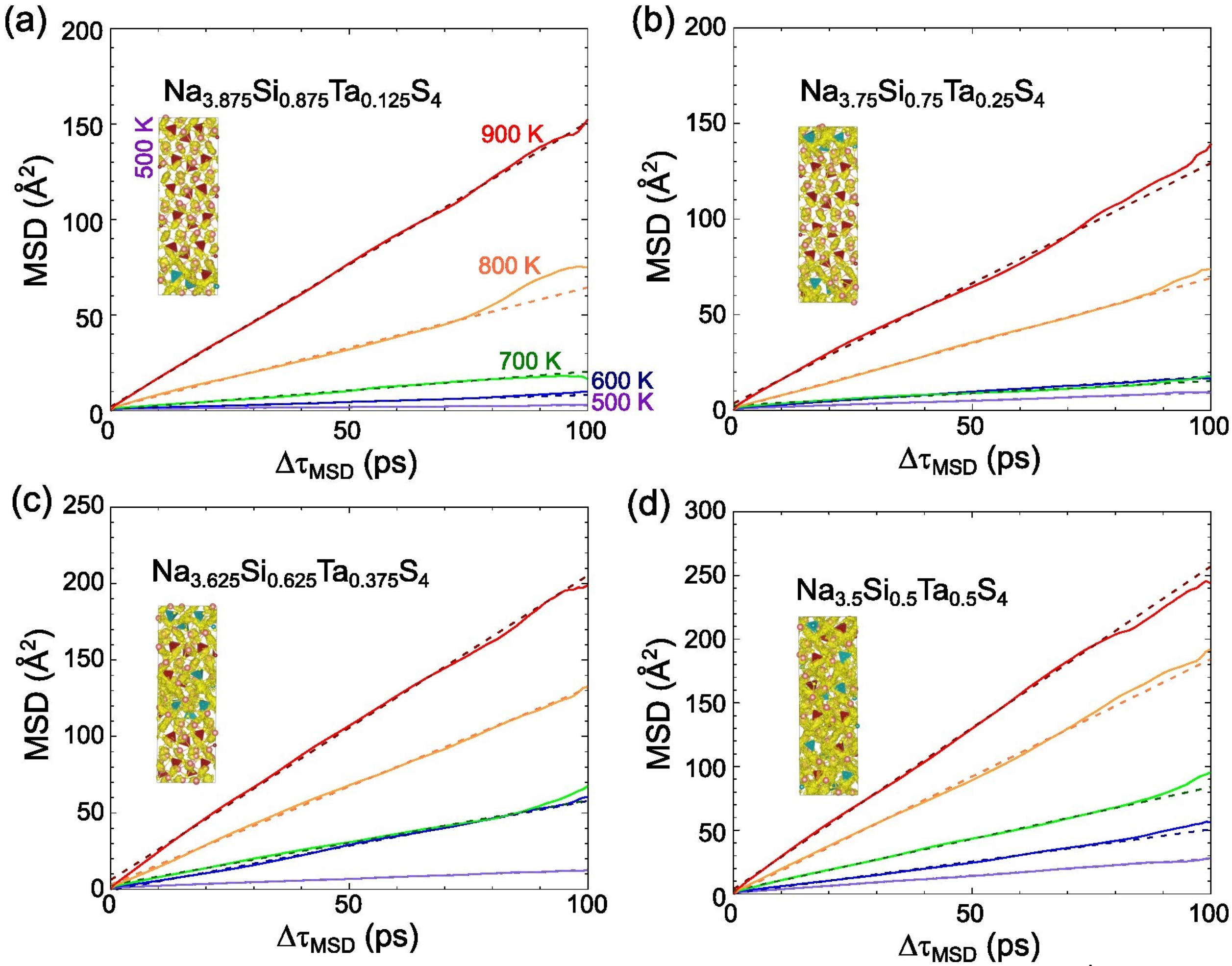

Figure S2 Mean squared displacement (MSD) curves against sampled time intervals $\Delta\tau_{MSD}$ given by the multi-temperature diagnosis (with $\Delta\tau = 1$ fs and $\tau = 100$ ps at $T = 500$, 600, 700, 800, and 900 K) for the four samples within $(M, M^{'},\Omega) = (Si, Ta, Na_4SiS_4)$: $Na_{3.875}Si_{0.875}Ta_{0.125}S_4$, $Na_{3.75}Si_{0.75}Ta_{0.25}S_4$, $Na_{3.625}Si_{0.625}Ta_{0.375}S_4$, and $Na_{3.5}Si_{0.5}Ta_{0.5}S_4$. For the MSD curves of Na_4SiS_4, Figure S1a is referred to. The dashed lines with slopes represent regression analyses, and the insets present the trajectory density plot at $T =$ 500 K represented by yellow isosurfaces.

Discussion S2 Electrochemical stability windows

We present the electrochemical stability windows and decomposition phases for the materials systems $(M, M^{'},\Omega) = (Ga, P, Na_4SiS_4)$ and (Si, Ta, Na_4SiS_4) in Table S3. These values were calculated using the Computational Phase Diagram App provided by MaterialsProject.org.[25, 26] The electrochemical stability window for $Na_4Ga_{0.125}Si_{0.75}P_{0.125}S_4$, $Na_4Ga_{0.25}Si_{0.5}P_{0.25}S_4$, $Na_4Ga_{0.375}Si_{0.25}P_{0.375}S_4$, $Na_4Ga_{0.5}P_{0.5}S_4$, $Na_{3.75}Ga_{0.375}P_{0.625}S_4$, and $Na_{4.25}Ga_{0.625}P_{0.375}S_4$ is $[1.24, 1.55]$ V vs. Na/Na$^+$, with multiple decomposition phases identified as Na_4SiS_4, Na_3GaS_3, Na_3PS_4, and Na_2S. When these decomposition phases form around solid interface regions, such as at the anode and cathode, the interphase-controlled electrochemical stability windows extend to $[0.77, 2.12]$ V vs. Na/Na$^+$.

Similarly, the electrochemical stability window for $Na_{3.875}Si_{0.875}Ta_{0.125}S_4$, $Na_{3.75}Si_{0.75}Ta_{0.25}S_4$, $Na_{3.625}Si_{0.625}Ta_{0.375}S_4$, and $Na_{3.5}Si_{0.5}Ta_{0.5}S_4$ is $[1.00, 1.91]$ V vs. Na/Na$^+$, with decomposition phases being Na_4SiS_4 and Na_3TaS_4. The interphase-controlled electrochemical stability window for these materials extends to $[0.77, 2.03]$ V versus Na/Na$^+$. Given that the narrow electrochemical stability windows for $(M, M^{'},\Omega) = (Ga, P, Na_4SiS_4)$ and (Si, Ta, Na_4SiS_4) are not significantly improved by interphase control, it is advisable to incorporate electrochemically stable interphase layers in battery design.[32] This is particularly important at the interfaces between the solid electrolyte and the anode, as well as between the solid electrolyte and the cathode.

Table S3. Electrochemical stability windows for the 11 compositions and decomposition phases adopted in the multi-temperature diagnosis.

Composition	Electrochemical stability windows (potential ϕ in V vs. Na/Na$^+$) (Corresponding decomposition phases if exist)
Na_4SiS_4	[0.77, 1.91]
$Na_4Ga_{0.125}Si_{0.75}P_{0.125}S_4$	[1.24, 1.55] (Na_4SiS_4, Na_3GaS_3, Na_3PS_4, Na_2S)
$Na_4Ga_{0.25}Si_{0.5}P_{0.25}S_4$	[1.24, 1.55] (Na_4SiS_4, Na_3GaS_3, Na_3PS_4, Na_2S)
$Na_4Ga_{0.375}Si_{0.25}P_{0.375}S_4$	[1.24, 1.55] (Na_4SiS_4, Na_3GaS_3, Na_3PS_4, Na_2S)
$Na_4Ga_{0.5}P_{0.5}S_4$	[1.24, 1.55] (Na_3GaS_3, Na_3PS_4, Na_2S)
$Na_{3.75}Ga_{0.375}P_{0.625}S_4$	[1.24, 1.55] (Na_3GaS_3, Na_3PS_4, Na_2S)
$Na_{4.25}Ga_{0.625}P_{0.375}S_4$	[1.24, 1.55] (Na_3GaS_3, Na_3PS_4, Na_2S)
$Na_{3.875}Si_{0.875}Ta_{0.125}S_4$	[1.00, 1.91] (Na_4SiS_4, Na_3TaS_4)
$Na_{3.75}Si_{0.75}Ta_{0.25}S_4$	[1.00, 1.91] (Na_4SiS_4, Na_3TaS_4)
$Na_{3.625}Si_{0.625}Ta_{0.375}S_4$	[1.00, 1.91] (Na_4SiS_4, Na_3TaS_4)
$Na_{3.5}Si_{0.5}Ta_{0.5}S_4$	[1.00, 1.91] (Na_4SiS_4, Na_3TaS_4)
Na_3GaS_3	[0.79, 1.65]
Na_3PS_4	[1.24, 2.12]
Na_2S	[0, 1.55]
Na_3TaS_4	[1.00, 2.03]

References

1. Harm, S.; Hatz, A.; Schneider, C.; Hoefer, C. A.; Hoch, C.; Lotsch, B. V. Finding the Right Blend: Interplay between Structure and Sodium Ion Conductivity in the System Na_5AlS_4-Na_4SiS_4. *Front. Chem.* **2020,** *8,* 90. DOI: 10.3389/fchem.2020.00090

2. Brown, A.; Tani, B. Powder X-Ray Diffraction Identification of Some New Phases in the Na_2S-Al_2S_3 System. *Mat. Res. Bull.* **1987,** 22 (8), 1029–1037. DOI: 10.1016/0025-5408(87)90231-5

3. Eisenmann, B.; Hofmann, A. Crystal Structure of Pentasodium Tetrathioindate(III), Na_5InS_4. *Z. Kristallogr. Crysta. Mater.* **1991,** *197* (1–2), 169–170. DOI: 10.1524/zkri.1991.197.1-2.169

4. Tanibata, N.; Noi, K.; Hayashi, A.; Tatsumisago, M. Preparation and Characterization of Highly Sodium Ion Conducting Na_3PS_4–Na_4SiS_4 Solid Electrolytes. *RSC Adv.* **2014,** *4* (33), 17120–17123. DOI: 10.1039/c4ra00996g

5. Tanibata, N.; Noi, K.; Hayashi, A.; Kitamura, N.; Idemoto, Y.; Tatsumisago, M. X-Ray Crystal Structure Analysis of Sodium-Ion Conductivity in $94Na_3PS_4{\cdot}6Na_4SiS_4$ Glass-Ceramic Electrolytes. *ChemElectroChem* **2014,** *1* (7), 1130–1132. DOI: 10.1002/celc.201402016

6. Tanibata, N.; Hayashi, A.; Tatsumisago, M. Improvement of Rate Performance for All-Solid-State $Na_{15}Sn_4$/Amorphous TiS_3 Cells Using $94Na_3PS_4{\cdot}6Na_4SiS_4$ Glass-Ceramic Electrolytes. *J. Electrochem. Soc.* **2015,** *162* (6), A793–A795. DOI: 10.1149/2.0011506jes

7. Heo, J. W.; Banerjee, A.; Park, K. H.; Jung, Y. S.; Hong, S. New Na-Ion Solid Electrolytes $Na_{4-x}Sn_{1-x}Sb_xS_4$ ($0.02 \leq x \leq 0.33$) for All-Solid-State Na-Ion Batteries. *Adv. Energy Mater.* **2018,** *8* (11), 1702716–1702716. DOI: 10.1002/aenm.201702716

8. Xiong, S.; Liu, Z.; Yang, L.; Ma, Y.; Xu, W.; Bai, J.; Chen, H. Anion and Cation Co-Doping of Na_4SnS_4 as Sodium Superionic Conductors. *Mater. Today Phys.* **2020,** *15,* 100281–100288. DOI: 10.1016/j.mtphys.2020.100281

9. Jumas, J.-C.; Philippot, E.; Vermot-Gaud-Daniel, F.; Ribes, M.; Maurin, M. Etude de la tétracoordination de l'etain dans deux orthothiostannates: Na_4SnS_4 et Ba_2SnS_4 (α). *J. Solid State Chem.* **1975,** *14* (4), 319–327. DOI: 10.1016/0022-4596(75)90050-x

10. He, Y.; Lu, F.; Kuang, X. Enhanced Sodium Ion Conductivity in Na_3VS_4 by P-Doping. *RSC Adv.* **2019,** *9* (67), 39180–39186. DOI: 10.1039/c9ra08900d

11. Peskov, M. V.; Blatov, V. A. Comparative Crystal-Chemical Analysis of *d*-Metal Sulfides, Selenides, and Tellurides and Binary Compounds. *Russ. J. Inorg.* **2006,** *51* (4), 590–598. DOI: 10.1134/s0036023606040140

12. Klepp, K. O.; Gabl, G. New Complex Sulfides of the VA-Metals: Preparation and Crystal Structure of Na_3VS_4 (With a Note on the Crystal Structure of the Low Temperature Modification of Na_3PO_4). *Eur. J. Solid State Inorg. Chem.* **1997,** *34* (10), 1143–1154.

13. Graf, H.; Schäfer, H. Zur Strukturchemie der Alkalisalze der Tetrathiosäuren der Elemente der 5. Hauptgruppe. *Z. Anorg. Allg. Chem.* **1976,** *425* (1), 67–80. DOI: 10.1002/zaac.19764250109.

14. Wang, H.; Chen, Y.; Hood, Z. D.; Sahu, G.; Amaresh Samuthira Pandian; Keum, J. K.; An, K.; Liang, C. An Air-Stable Na_3SbS_4 Superionic Conductor Prepared by a Rapid and Economic Synthetic Procedure. *Angew. Chem.* **2016,** *55* (30), 8551–8555. DOI: 10.1002/anie.201601546

15. Banerjee, A.; Park, K. H.; Heo, J. W.; Nam, Y. J.; Moon, C. K.; Oh, S. M.; Hong, S.-T.; Jung, Y. S. Na_3SbS_4: A Solution Processable Sodium Superionic Conductor for All-Solid-State Sodium-Ion Batteries. *Angew. Chem. Int. Ed.* **2016,** *55* (33), 9634–9638. DOI: 10.1002/anie.201604158

16. Ewald, P. P. Die Berechnung Optischer und Elektrostatischer Gitterpotentiale. *Ann. Phys.* **1921,** *369* (3), 253–287. DOI: 10.1002/andp.19213690304

17. Toukmaji, A. Y.; Board, J. A. Ewald Summation Techniques in Perspective: A Survey. *Comput. Phys. Commun.* **1996,** *95* (2–3), 73–92. DOI: 10.1016/0010-4655(96)00016-1

18. Jang, S.; Jalem, R.; Tateyama, Y. *EwaldSolidSolution:* A High-Throughput Application to Quickly Sample Stable Site Arrangements for Ionic Solid Solutions. *J. Phys. Chem. A* **2023,** *127* (27), 5734–5744. DOI: 10.1021/acs.jpca.3c00076

19. Blöchl, P. E. Projector Augmented-Wave Method. *Phys. Rev. B* **1994**, *50* (24), 17953-17979. DOI: 10.1103/PhysRevB.50.17953

20. Perdew, J. P.; Burke, K.; Ernzerhof, M. Generalized Gradient Approximation Made Simple. *Phys. Rev. Lett.* **1996**, *77* (18), 3865-3868. DOI: 10.1103/PhysRevLett.77.3865

21. Kresse, G.; Furthmüller, J. Efficiency of Ab-initio Total Energy Calculations for Metals and Semiconductors Using a Plane-Wave Basis Set. *Comp. Mater. Sci.* **1996**, *6* (1), 15-50. DOI: 10.1016/0927-0256(96)00008-0

22. Kresse, G.; Furthmüller, J. Efficient Iterative Schemes for Ab Initio Total-Energy Calculations Using a Plane-Wave Basis Set. *Phys. Rev. B* **1996**, *54* (16), 11169-11186. DOI: 10.1103/PhysRevB.54.11169

23. Kresse, G.; Joubert, D. From Ultrasoft Pseudopotentials to the Projector Augmented-Wave Method. *Phys. Rev. B* **1999**, *59* (3), 1758-1775. DOI: 10.1103/PhysRevB.59.1758

24. Monkhorst, H. J.; Pack, J. D. Special Points for Brillouin-Zone Integrations. *Phys. Rev. B* **1976**, *13* (12), 5188-5192. DOI: 10.1103/PhysRevB.13.5188

25. Ong, S. P.; Wang, L.; Kang, B.; Ceder, G. The Li-Fe-P-O_2 Phase Diagram from First Principles Calculations. *Chem. Mater.* **2008,** *20* (5), 1798-1807. DOI: 10.1021/cm702327g

26. Ong, S. P.; Jain, A.; Hautier, G.; Kang, B.; Ceder, G. Thermal Stabilities of Delithiated Olivine MPO_4 (M=Fe, Mn) Cathodes Investigated Using First Principles Calculations. *Electrochem. commun.* **2020,** *12* (3), 427-430. DOI: 10.1016/j.elecom.2010.01.010

27. Heyd, J.; Scuseria, G. E.; Ernzerhof, M. Hybrid Functionals Based on a Screened Coulomb Potential. *J. Chem. Phys.* **2003,** *118* (18), 8207–8215. DOI: 10.1063/1.1564060

28. Nosé, S. A Unified Formulation of the Constant Temperature Molecular Dynamics Methods. *J. Chem. Phys.* **1984,** *81* (1), 511-519. DOI: 10.1063/1.447334

29. Hoover, W. G. Canonical Dynamics: Equilibrium Phase-Space Distributions. *Phys. Rev. A* **1985,** *31* (3), 1695-1697. DOI: 10.1103/PhysRevA.31.1695

30. Parrinello, M.; Rahman, A. Crystal structure and pair potentials: a molecular-dynamics study. *Phys. Rev. Lett.* **1980,** *45* (14), 1196-1199. DOI: 10.1103/PhysRevLett.45.1196

31. Parrinello, M.; Rahman, A. Polymorphic transitions in single crystals: a new molecular dynamics method. *J. Appl. Phys.* **1981,** *52* (12), 7182-7190. DOI: 10.1063/1.328693

32. Niu, Y.; Yu, Z.; Zhou, Y.; Tang, J.; Li, M.; Zhuang, Z.; Yang, Y.; Huang, X.; Tian, B. Constructing stable Li-solid electrolyte interphase to achieve dendrites-free solid-state battery: A nano-interlayer/Li pre-reduction strategy. *Nano Res.* **2022,** *15* (8), 7180-7189. DOI: 10.1007/s12274-022-4362-y